Prace Naukowe Instytutu Maszyn, Napędów i Pomiarów Elektrycznych
Nr 65 Politechniki Wrocławskiej Nr 65

Studia i Materiały Nr 31 2011

variable speed drives, induction motor,
vector control, sensorless control, estimators

Mateusz DYBKOWSKI, Teresa ORŁOWSKA-KOWALSKA,
Grzegorz TARCHAŁA*

PERFORMANCE ANALYSIS OF THE SPEED SENSORLESS INDUCTION MOTOR DRIVE WITH MAGNETIZING REACTANCE ESTIMATOR

In this paper the sensorless induction motor drive performance with current-based MRAS speed and rotor flux estimator are tested in the wide speed range operation. This system has been equipped with additional estimator of the magnetizing reactance reconstruction. Methodology is based on the well known mathematical interpolation of the inverse magnetizing curve. Dynamical performances of the vector control system with such this current-type MRAS estimator with magnetizing reactance on-line adaptation are tested in simulation and experiments.

1. INTRODUCTION

The universal speed sensorless induction motor drive should work stable for starting from the standstill, for low speed region and in the regenerating mode [2], [3], [6], [10]. Control structure should assure good dynamical performance in the wide speed reference changes (including a field weakening region).

One of the most popular solutions of the speed and flux reconstruction is the MRAS (Model Reference Adaptive System) methodology presented first in [4], [8], [9]. However, a classical rotor-flux-based MRAS estimator is sensitive to motor parameter changes due to the high sensitivity of rotor flux current and voltage models used for rotor flux vector estimation. Nevertheless this methodology is still developed. The current-type MRAS type speed and flux estimator [1], [7] is less sensitive to the motor parameters changes than classical solutions and is stable for the whole reference speed changes.

* Wrocław University of Technology, Institute of Electrical Machines, Drives and Measurements, ul. Smoluchowskiego 19, 50-372 Wrocław, e-mail: mateusz.dybkowski@pwr.wroc.pl, teresa.orlowska-kowalska@pwr.wroc.pl, grzegorz.tarchala@pwr.wroc.pl

It was proved however, that all speed estimators are sensitive to changes of the magnetizing reactance of the induction motor. Magnetizing reactance of the induction motor depends on the magnetizing flux and current. Its value is not constant during the motor operation in the control structure [5], so the speed estimator should be extended with the estimator of this parameter.

In this paper the sensorless Direct Field Oriented Control structure of the induction motor is tested. The speed and rotor flux reconstruction is based on the MRAS^{CC} [1], [7] estimator, equipped with magnetizing reactance estimator, according to the methodology presented in [5], [11]. Sensitivity of the drive system to the magnetizing reactance for different speed values is checked. Dynamical performances are investigated in the whole speed range, including the field weakening and low speed regions (typical for the traction and Electrical Vehicle (EV) drives).

2. IDENTIFICATION ALGORITHM OF THE MAGNETIZING REACTANCE

Parameters of the induction motor are not constant under the drive system operation and they depend on the temperature, current and motor speed. One of the most important parameter in the sensorless induction motor drive, which influences its behavior, is a magnetizing reactance. This parameter in the field weakening region is bigger than its nominal value. So the structure of the speed and flux estimator used in sensorlees drive should be modified by estimated magnetizing reactance.

The magnetizing reactance can be calculated from the equation:

$$x_m = \frac{\Psi_m}{i_m} \tag{1}$$

where the magnetizing flux vector can be obtained from:

$$\Psi_m = \sqrt{\Psi_{m\alpha}^2 + \Psi_{m\beta}^2} \tag{2}$$

and:

$$\begin{aligned} \Psi_{m\alpha} &= \int \left(u_{s\alpha} - r_s i_{s\alpha}\right) dt - x_{\sigma s} i_{s\alpha} \\ \Psi_{m\beta} &= \int \left(u_{s\beta} - r_s i_{s\beta}\right) dt - x_{\sigma s} i_{s\beta} \end{aligned} \tag{3}$$

The magnetizing current depends on the rotor current and can be calculated as follows:

$$\begin{aligned} i_{m\alpha} &= i_{s\alpha} + i_{r\alpha} \\ i_{m\beta} &= i_{s\beta} + i_{r\beta} \end{aligned} \tag{4}$$

All variables in (1)–(4) are expressed in the stator coordinate system. Rotor current cannot be measured in the control structures, so the magnetizing current can be estimated using the known nonlinear inverse magnetizing curve:

$$i_m = f(\Psi_m) \tag{5}$$

$$x_m^{est} = \frac{\Psi_m}{i_m} \tag{6}$$

It should be mentioned, that the linear mathematical model of IM and classical coordinate transformation to α–β components has been used, despite the nonlinearity of magnetizing characteristics (5). But it is commonly applied approach [5], and in the case of analysed in this paper, the compatibility of simulation and experimental test confirms the correctness of this approach.

Magnetizing curve can be represented in per unit as in [8]:

$$i_m = a\Psi_m + (1-a)\Psi_m^b \tag{7}$$

where a and b are determined as constant coefficients characteristic for the given induction motor.

As it is presented in [5], estimated magnetizing current depends on the coefficients a and b. Proper choice of those values guaranties the good reconstruction of this current versus magnetizing flux. In the Fig. 1 the magnetizing curves for different values of parameters a and b are shown.

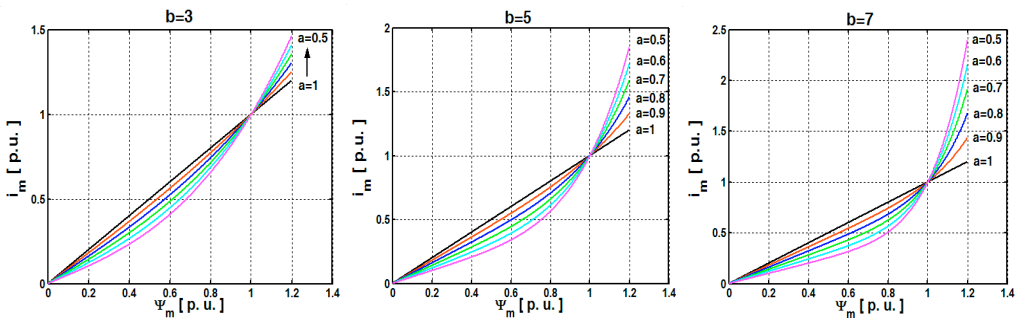

Fig. 1. The magnetizing curves of an induction motor for different values of parameters a and b

It was presented in [5], [11] that for low and medium power induction motors, parameter b should be equal to 7 and parameter a should be set between 0.6 and 0.9.

The magnetizing curve and the magnetizing reactance variation of the induction motor tested in this paper (with parameters presented in detail in Appendix) are shown in Fig. 2. The calculated curves are compared with the measured characteristics. Coefficients a and b were determined as $a = 0.7$ and $b = 7$. The measured points are marked with cross, while the calculated ones are marked by dot. It is seen from this compari-

son, that a very good accuracy of the measured magnetizing curve is obtained with the characteristic given by (7), according to the methodology proposed in [5].

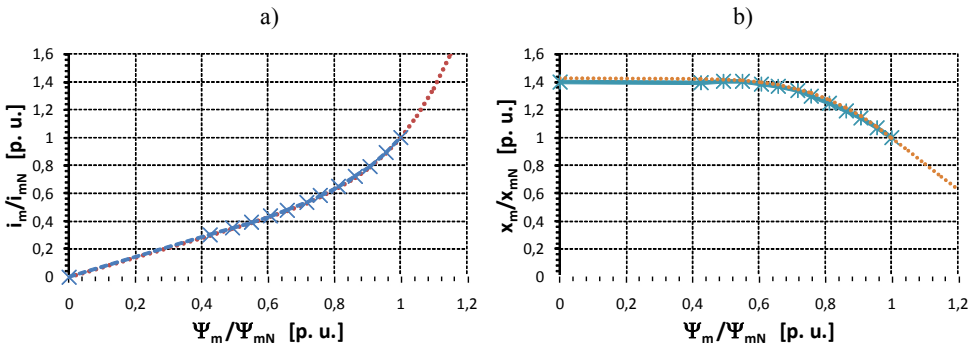

Fig. 2. Magnetizing curve (a) and magnetizing reactance (b) variation of the machine used in simulation and experiments (a = 0.7 and b = 7)

3. MATHEMATICAL MODEL OF THE MRAS^{CC} ESTIMATOR

The MRAS^{CC} estimator was presented in detail in a paper [7]. It is based on two well known simulators [6] (voltage model and current model of rotor flux) transformed to the stator current estimator and to the rotor flux estimator based on a current model.

Current estimator used in MRAS^{CC} is obtained by the equation:

$$\frac{d}{dt}\mathbf{i}_s^e = -\frac{r_r x_m^2 + x_r^2 r_s}{\sigma T_N x_s x_r^2}\mathbf{i}_s^e + \frac{1}{\sigma T_N x_s}\mathbf{u}_s + \frac{x_m r_r}{\sigma T_N x_s x_r^2}\boldsymbol{\Psi}_r^i - j\omega_m^e \frac{x_m}{\sigma T_N x_s x_r}\boldsymbol{\Psi}_r^i \tag{8}$$

where: ω_m^e – estimated rotor angular speed, r_s, r_r, x_s, x_r, x_m – stator and rotor resistances, stator and rotor leakage reactances, $\mathbf{u}_s$, $\mathbf{i}_s^e$, $\boldsymbol{\Psi}_r^i$ – stator voltage, estimated stator current and rotor flux vectors respectively, $\sigma = 1 - x_m^2/x_s x_r$, $T_N = 1/2\pi f_{sN}$, f_{sN} – nominal frequency. Current model can be calculated from the equation:

$$\frac{d}{dt}\boldsymbol{\Psi}_r^i = \left[\frac{r_r}{x_r}(x_m\mathbf{i}_s - \boldsymbol{\Psi}_r^i) + j\omega_m^e\boldsymbol{\Psi}_r^i\right]\frac{1}{T_N} \tag{9}$$

Both stator current model (8) and rotor flux model (9) are adjusted by the estimated rotor speed [4]:

$$\omega_m^e = K_P(e_{i_{s\alpha}}\Psi_{r\beta}^i - e_{i_{s\beta}}\Psi_{r\alpha}^i) + K_I\int(e_{i_{s\alpha}}\Psi_{r\beta}^i - e_{i_{s\beta}}\Psi_{r\alpha}^i)\,dt \tag{10}$$

where $e_{i_{s\alpha,\beta}} = i_{s\alpha,\beta} - i_{s\alpha,\beta}^e$ – error between the estimated and measured stator current.

The MRAS^{CC} estimator can be extended with the magnetizing reactance estimator presented in the Chapter 2. The general scheme of the MRAS^{CC} estimator with on-line magnetizing reactance estimation algorithm is presented in Fig. 3.

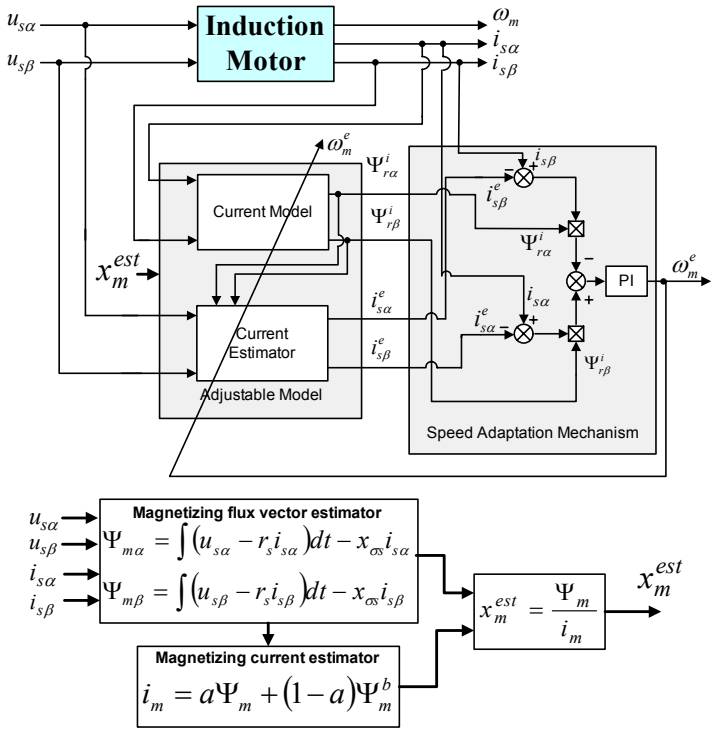

Fig. 3. MRAS^{CC} estimator with magnetizing reactance estimator

The MRAS^{CC} speed and rotor flux estimator is robust to the all motor parameters changes and is stable in the whole speed reference changes [1]. Stability and sensitivity analysis were presented in detail in [7]. From those analyses results, that the magnetizing reactance should be perfectly known (or identified on-line), when the drive system is operating in the wide speed range.

4. SIMULATION TESTS OF THE DRIVE SYSTEM

Direct Field Oriented Control structure with MRAS^{CC} estimator and reactance estimator used in simulation and experimental set up is presented in Fig. 4. In this chapter chosen simulation results are shown.

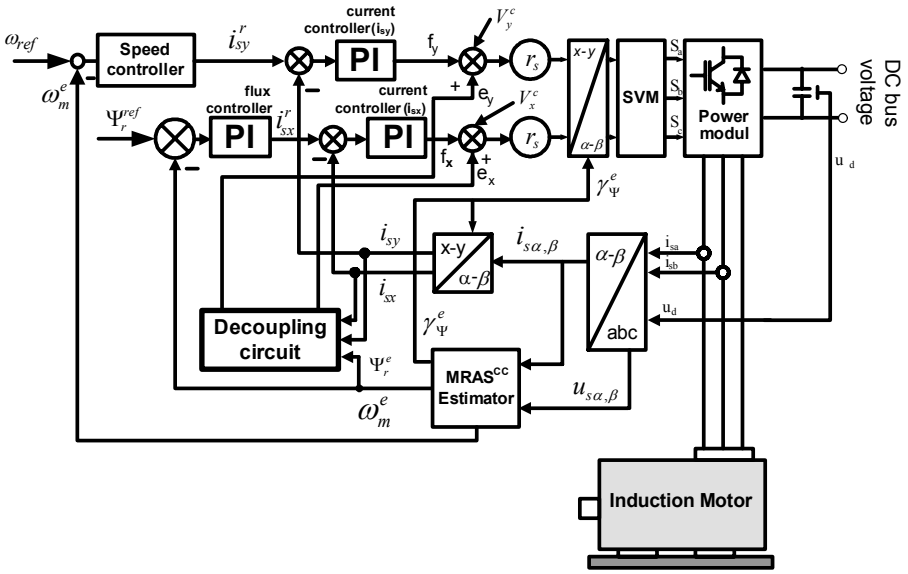

Fig. 4. Sensorless speed control structure

First, the performance of the sensorless drive without magnetizing reactance updating in the field weakening region are shown in Fig. 5 and Fig. 6. The sensorless IM drive works properly. But in the steady state, for the speed references bigger than nominal, $\omega_m = 1.5\omega_{mN}$, the small error between the measured and estimated speed is

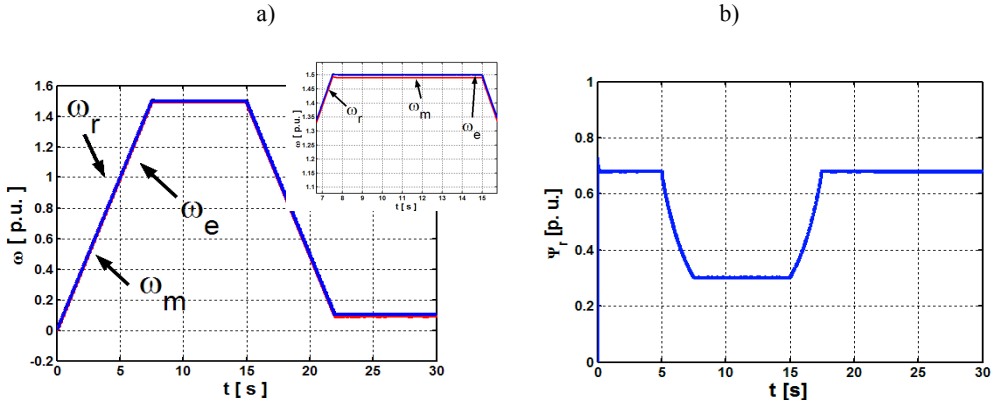

Fig. 5. Transients of the sensorless IM drive for the field weakening and in the low speed region without magnetizing reactance estimator

visible (Fig. 5a, Fig. 6b). This error is connected with the wrong magnetizing reactance value, used in the speed estimator mathematical model. This value increases for such high motor speed due to a flux weakening. If the magnetizing reactance is not estimated, speed reconstruction error oscillates around zero only for the rotor speed smaller than its nominal value; for higher speed, especially for the loaded motor, the steady state error is visible. Components i_{sx} and i_{sy} of the stator current vector depend respectively on the rotor flux vector magnitude and electromagnetic torque in the DFOC structure, and are demonstrated in Fig. 6c.

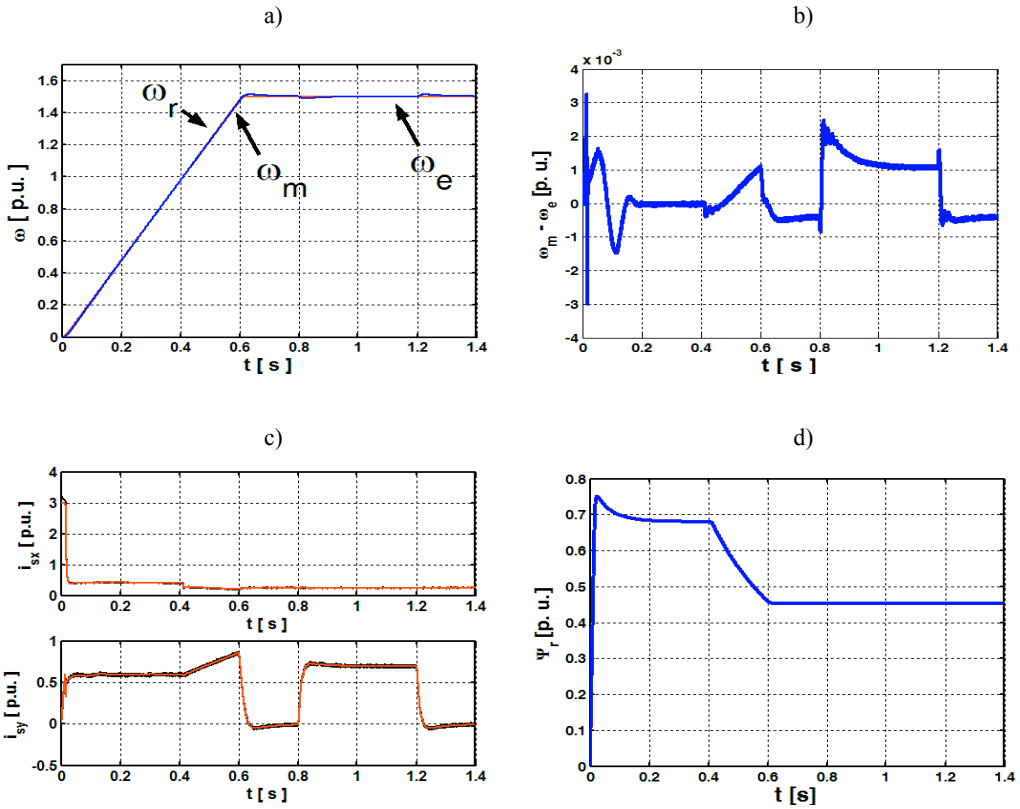

Fig. 6. Simulation results of the sensorless IM drive with MRAS^{CC} estimator without magnetizing reactance estimator for the field weakening region

The steady-state speed estimation error is cancelled in the control structure with MRAS^{CC} speed and flux estimator, extended with the magnetizing reactance estimator. The rotor speed is reconstructed in the whole speed reference properly (Fig. 7a). Speed estimation error oscillates around zero value (see Fig. 7b).

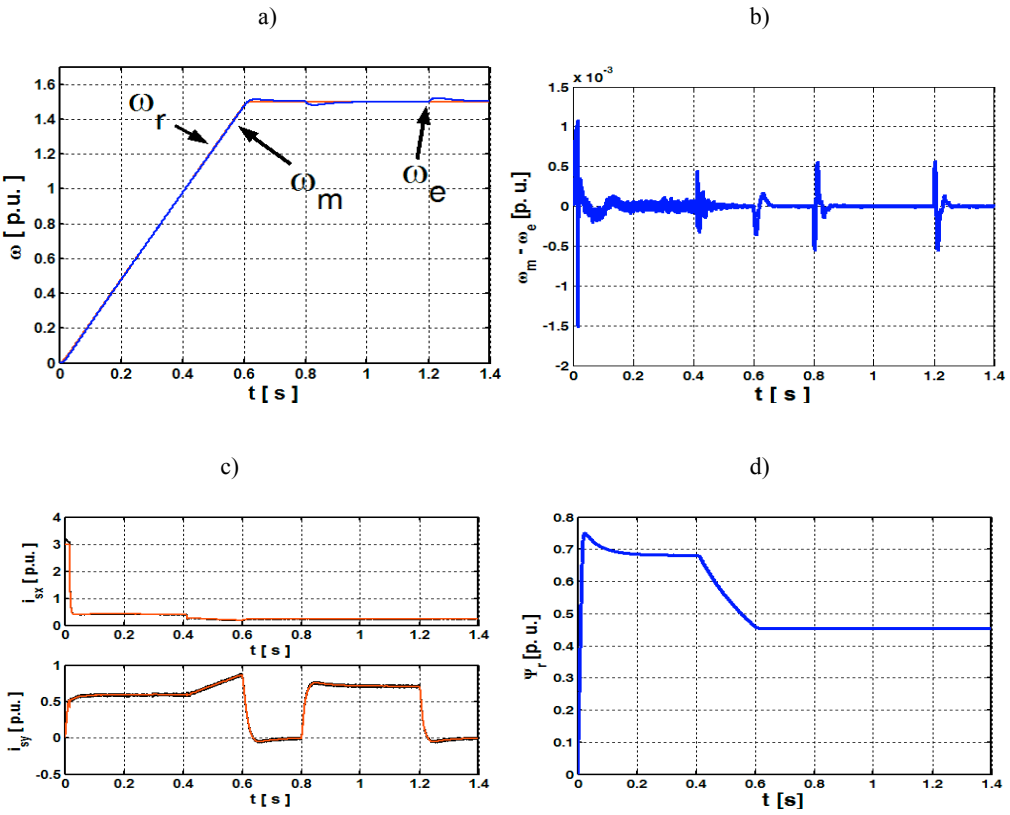

Fig. 7. Simulation results of the sensorless IM drive with MRAS^{CC} estimator with magnetizing reactance estimator for the field weakening region

5. CHOSEN EXPERIMENTAL RESULTS

Proposed estimation algorithm and DFOC control structure was implemented in the laboratory set-up with PC computer, using the dSPACE software. The schematic diagram of the experimental test bench is shown in Fig. 8. The experimental set-up is composed of the IM motor fed by voltage inverter with Space Vector Modulator (SVM). The motor is coupled to a load machine (AC motor supplied from an AC inverter). The driven motor has the nominal power of 1.1 kW. The speed and position of the drive are measured by the incremental encoder (5000 imp./rev), only for the comparison with the estimated speed in the sensorless drive. The control and estimation algorithms are implemented in DS1103 card.

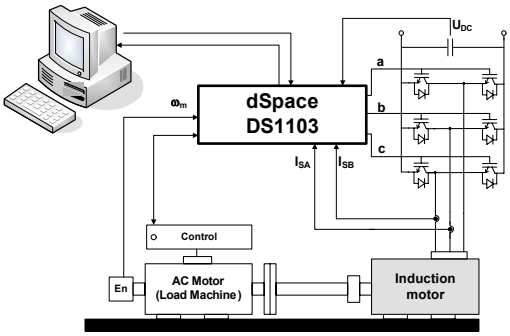

Fig. 8. Schematic diagram of the laboratory test bench

In the Figures 9 and 10 the chosen experimental result of the sensorless IM drive under different condition are demonstrated. First, the operation of sensorless DFOC system based on MRAS^{CC} estimator without additional magnetizing reactance adaptation is shown in Fig. 9. A steady-state speed estimation error is observed.

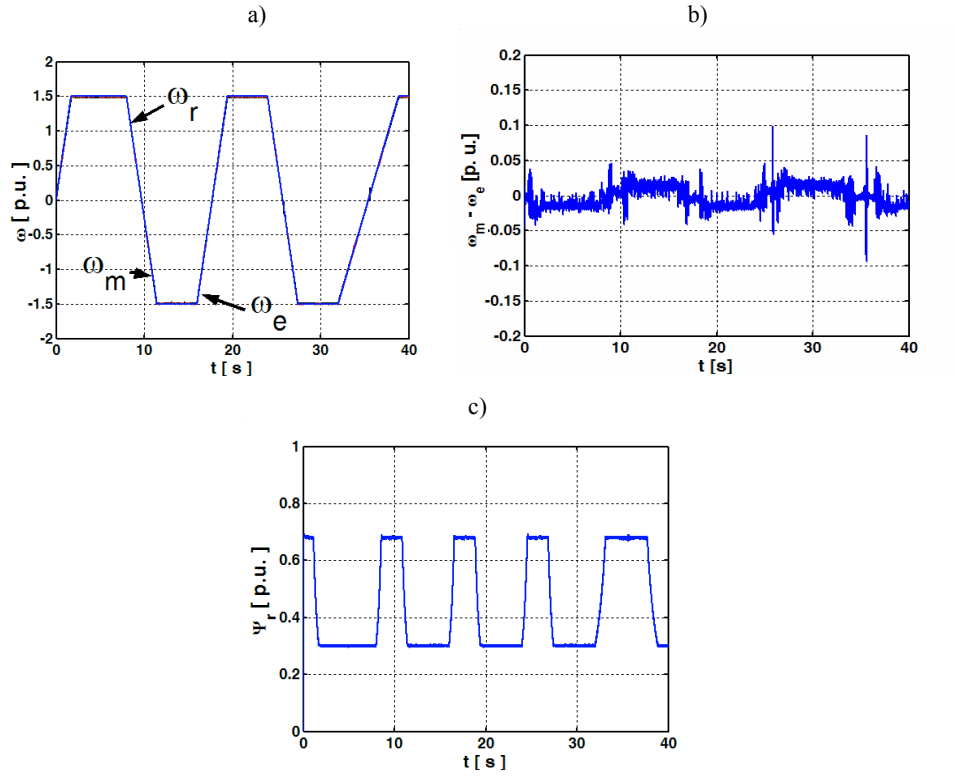

Fig. 9. Experimental results of the sensorless IM drive with MRAS^{CC} speed and flux estimator for the field weakening and small speed region without magnetizing reactance estimator

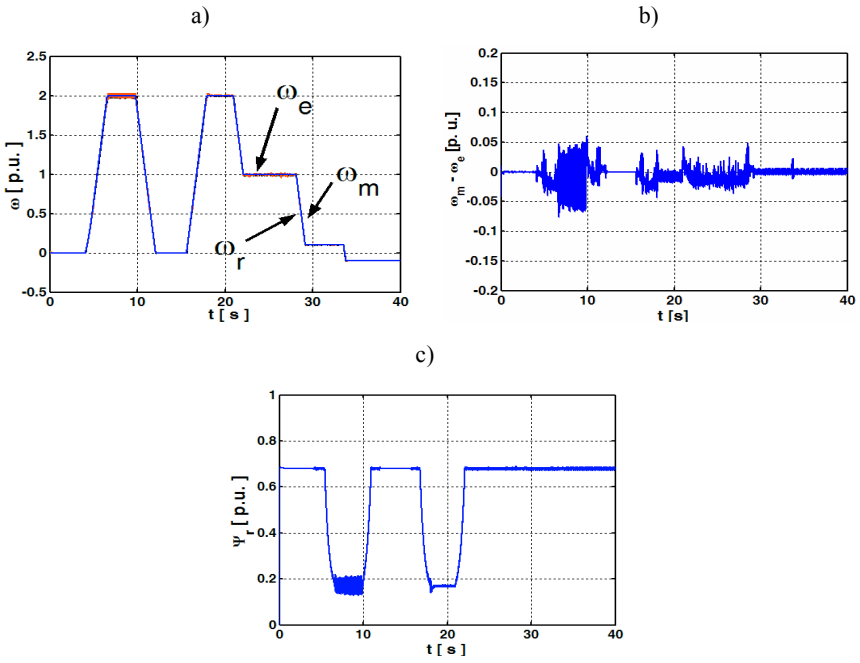

Fig. 10. Experimental results of the sensorless IM drive with MRAS^{CC} speed and flux estimator for the field weakening and small speed region with magnetizing reactance estimator

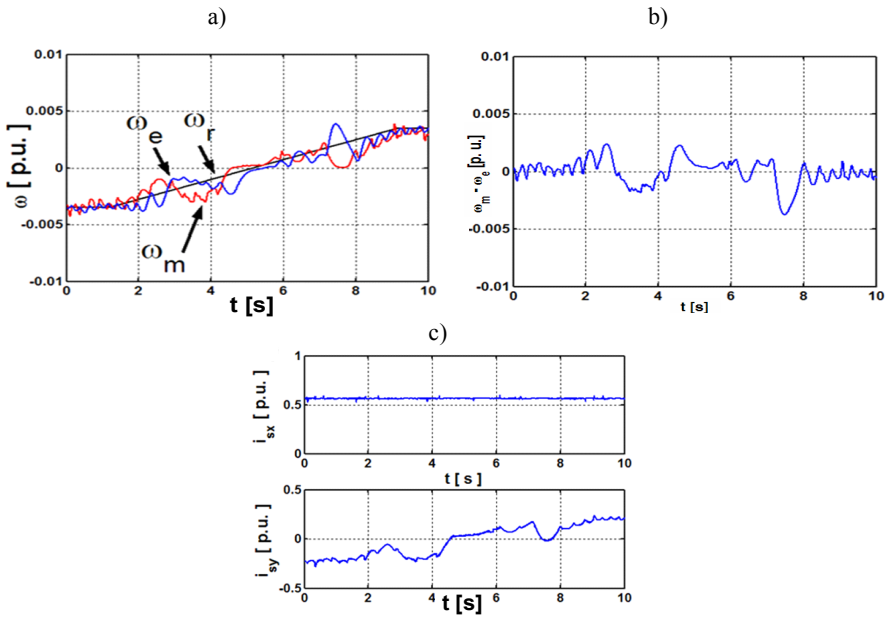

Fig. 11. Experimental results of the sensorless IM drive with MRAS^{CC} speed and flux estimator for the reverse operation from the speed reference $\omega_{\text{ref}} = -0.0035\omega_{mN}$ to $\omega_{\text{ref}} = 0.0035\omega_{mN}$, $m_{oL} = 0.25m_N$

Next sensorless drive with MRAS^{CC} estimator equipped with the proposed magnetizing reactance estimation algorithm is tested and results are shown in Fig. 10. Drive system works properly in the field weakening region and an average value of the speed estimation error (Fig. 10b) is now close to zero.

In Figure 11 a very long reverse operation under load torque in a small speed region of the sensorless drive is shown. It can be seen that the drive works properly. Small speed error is visible only for a speed reference close to zero. It proves that the updating of the magnetizing reactance improves the drive system operation in the whole speed range, from very low, through nominal, to much higher than nominal value.

6. CONCLUSIONS

The MRAS^{CC} speed and flux estimator, which uses the current model and current estimator, performs very well in the wide range of the speed reference, in the sensorless DFOC drive system. When using the proposed estimation algorithm of the magnetizing reactance, steady state performance of the drive can be improved, as the small speed estimation errors in field weakening region as well in a very low speed region are completely removed. This estimation algorithm of the magnetizing reactance can be easily implemented in the MRAS^{CC} estimator. Control structure with the analyzed estimator can be implemented in the drive working with very low and high speeds.

APPENDIX

Motor rated data

P_N = 1.1 [kW] U_N = 230/400[V] I_N = 5.0/2.9 [A]	n_N = 1380 [rpm] f_N = 50 [Hz] p_b = 2

Parameters of the IM equivalent circuit

R_s	R_r	X_s	X_r	X_m	
5.9	4.5	131.1	131.1	123.3	[Ω]
0.07	0.06	1.725	1.725	1.62	[p.u.]

Per unit system calculation methodology (reference values):

$U_b = \sqrt{2}\, U_{Nf},\ I_b = \sqrt{2}\, I_N,\ Z_b = U_b/I_b,\ \omega_b = 2\pi f_N,\ \Psi_b = U_b/\omega_b,\ S_b = (3/2)U_b I_b,\ M_b = S_b p_b/\omega_b,$

Parameters in per unit system:

$r_s = R_s/Z_b,\ r_r = R_r/Z_b,\ x_s = l_s = X_s/Z_b,\ x_r = l_r = X_r/Z_b,\ x_m = l_m = X_m/Z_b$

REFERENCES

[1] DYBKOWSKI M., ORŁOWSKA-KOWALSKA T., *Application of the Stator Current-based MRAS Speed Estimator in the Sensorless Induction Motor Drive*, Proc. of 13th Confer. EPE–PEMC 2008, Poznań, Poland, on CD, 2008.

[2] HOLTZ J., *Sensorless Control of Induction Machines – With or Without Signal Injection?*, IEEE Trans. Industrial Electronics, Vol. 53, No. 1, 2006, pp. 7–30.

[3] KAZMIERKOWSKI M.P., BLAABJERG F., KRISHNAN, *Control In Power Electronic – Selected Problems*, Academic Press, USA, 2002

[4] KUBOTA H., MATSUSE K., NAKANO T., *New adaptive flux observer for wide speed range motor drives*, Proc. Int. Confer. IEEE-IECON'1990, pp. 921–926.

[5] LEVI E., SOKOLA M., VUKOSAVIC S.N., *A Method for Magnetizing Curve Identification in Rotor Flux Oriented Induction Machines*, IEEE Trans. Energy Conversion, 2000, Vol. 15, No. 2, pp. 157–162.

[6] ORŁOWSKA-KOWALSKA T., *Bezczujnikowe układy napędowe z silnikami indukcyjnymi*, Oficyna Wydawnicza Politechniki Wrocławskiej, Wrocław 2003.

[7] ORŁOWSKA-KOWALSKA T., DYBKOWSKI M., *Stator Current-based MRAS Estimator for Wide Range Speed-Sensorless Induction Motor Drive*, IEEE Trans. on Industrial Electronics, 2010, Vol. 57, No. 4, pp. 1296–1308.

[8] SCHAUDER C., *Adaptive speed identification for vector control of induction motors without rotational transducers*, IEEE Trans. Industry Applications, 1992, Vol. 28, No. 5, pp. 1054–1061.

[9] TAMAI S., SUGIMOTO H., MASAO Y., *Speed Sensorless Vector Control of Induction Motor with Model Reference Adaptive System*, Proc. of IEEE'/IAS, 1987, pp. 189–195.

[10] VAS P., *Sensorless vector and direct torque control*, Oxford University Press, New York 1998.

[11] ZAKY M. S., KHATER M.M., SHOKRALLA S.S., YASIN H.A., *Wide-Speed-Range Estimation With Online Parameter Identification Schemes of Sensorless Induction Motor Drives*, IEEE Trans. Industrial Electronics, 2009, Vol. 56, No. 5, pp. 1699–1707.